Supporting Information

2D Spin Glass $MnIn_2Se_4$: Application of Liquid-Phase Exfoliation to a Layered Structure with Seven-Atom-Thick Layers

Govind Sasi Kumar,[a] Yan Xin,[b] J. S. Raaj Vellore Winfred,[a] Judith K. Clark,[a] and Michael Shatruk*[,a,b]

[a] *Department of Chemistry and Biochemistry, Florida State University, Tallahassee, FL 32306, United States*
[b] *National High Magnetic Field Laboratory, Tallahassee, FL 32310, United States*

*Corresponding authors: shatruk@chem.fsu.edu

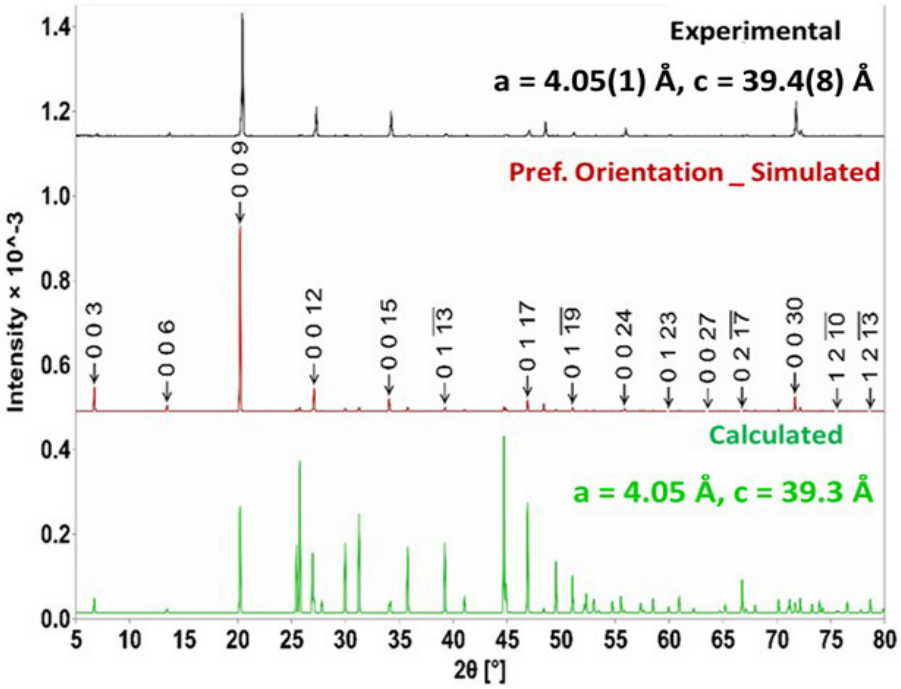

Figure S1. Powder X-ray diffraction patterns of bulk $MnIn_2Se_4$ (black), compared to the calculated patterns with (red) and without (green) preferred orientation along the [00*l*] direction.

Table S1. Results of exfoliation of $MnIn_2Se_4$ crystals in different solvents.

Solvent	Surface Tension (N/m)	Result of Exfoliation
Isopropanol	0.023	Stable suspension*
Ethanol	0.022	Unstable suspension
Acetone	0.024	Unstable suspension
NMP	0.042	Unstable suspension
Water	0.072	Unstable suspension

* The sheets exfoliated by ultrasonication in isopropanol were isolated by size-selective centrifugation performed at speeds of 2000, 5000, and 7500 rpm. Energy-dispersive X-ray analysis carried out on the samples obtained at these centrifugation speeds gave Mn:In:Se ratios of 0.95:2:4, 0.9:2:4, and 0.9:2:4, respectively.

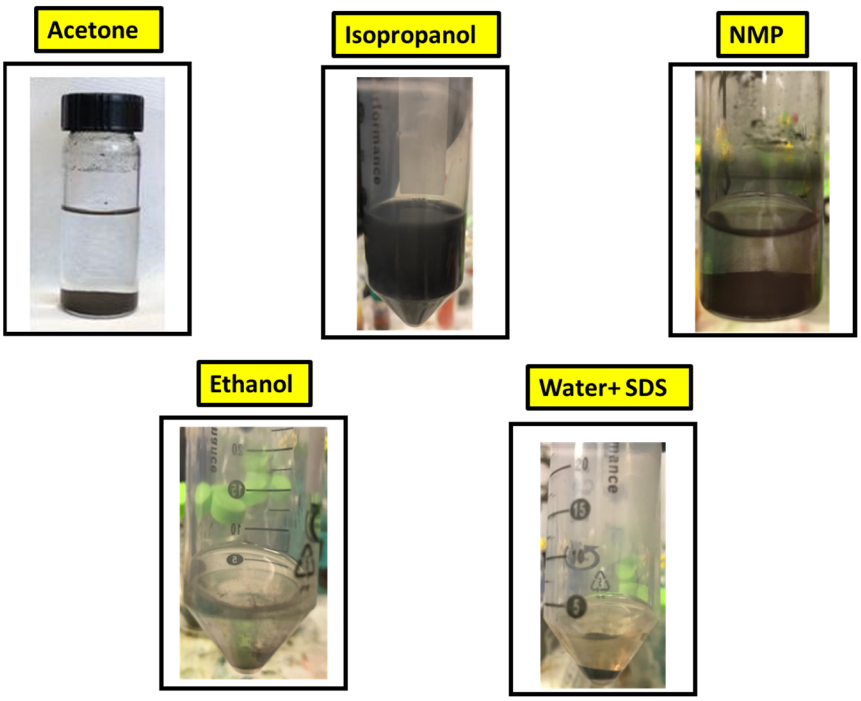

Figure S2. Images of the exfoliated sheets of $MnIn_2Se_4$ in various solvents two days after ultrasonication. Only the suspension of sheets in isopropanol was stable for a prolonged period, while relatively fast precipitation of sheets was observed with other solvents.

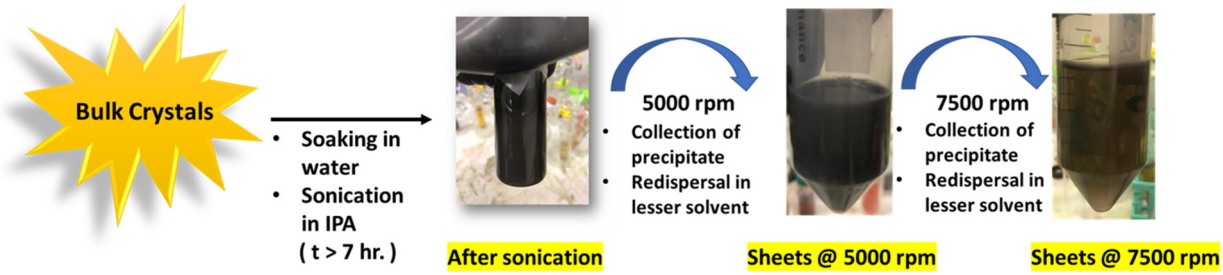

Figure S3. Schematic representation of the liquid phase exfoliation of $MnIn_2Se_4$ crystals. The sheets isolated at the centrifugation speeds of 5000 and 7500 rpm were taken for further studies.

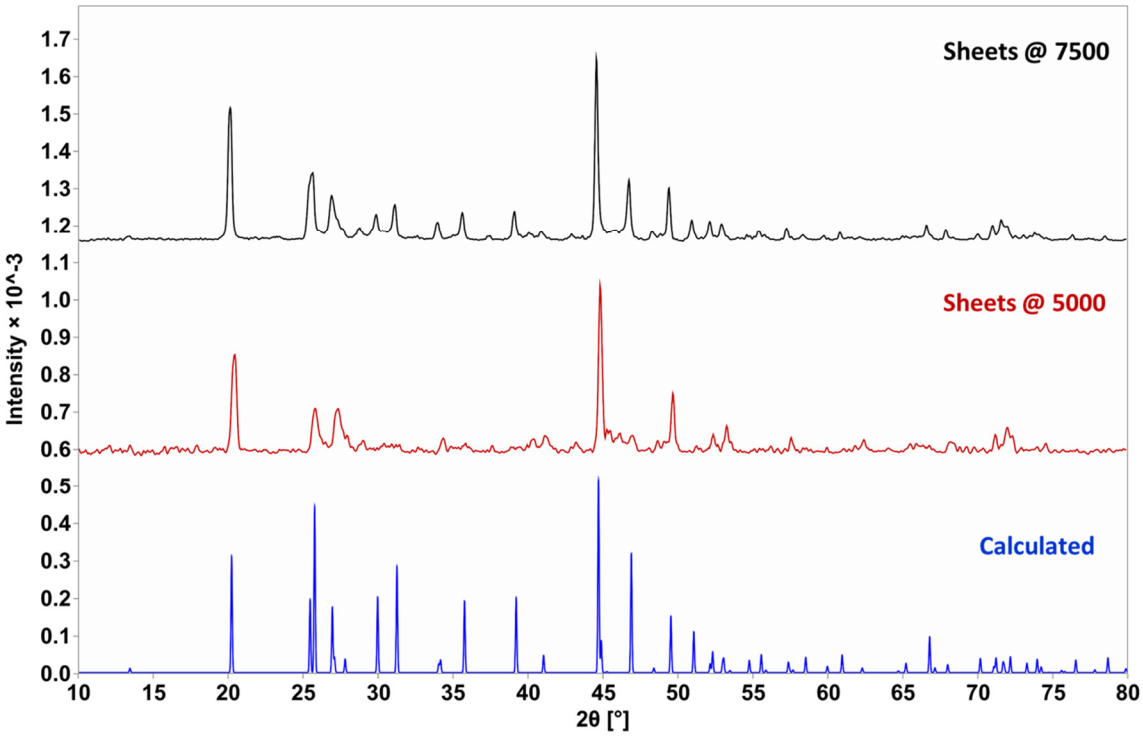

Figure S4. PXRD patterns of exfoliated $MnIn_2Se_4$ sheets isolated at 5000 rpm (red) and 7500 rpm (black) and the pattern calculated from the crystal structure of $MnIn_2Se_4$ (blue).

Estimating the thickness of nanosheets by EELS

The thicknesses of the flakes were measured in the TEM diffraction mode at the 8 cm camera length. The probe convergence semi-angle was 4 mrad and the collection semi-angle was about 30 mrad. The effective atomic number was calculated to be 37. The thickness was calculated by the log-ratio method using ZLP in Gatan DigitalMicrograph software. The carbon support film is ~10 nm thick. Therefore, all calculated thicknesses were corrected by subtracting this value to obtain the real thickness of nanosheets.

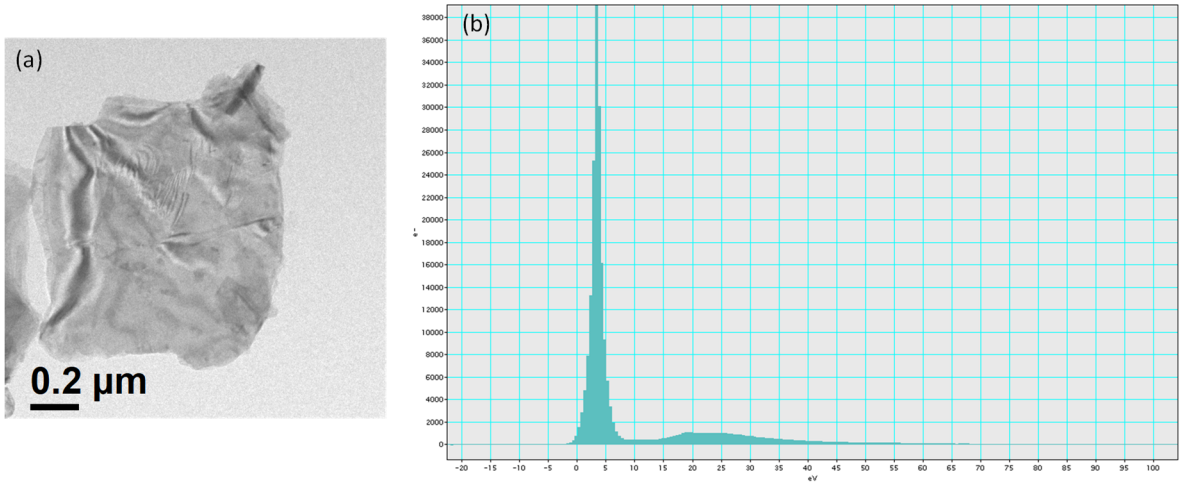

Figure S5. A TEM bright-field image of a selected nanosheet (a) and its EELS zero loss peak spectrum (b). The calculated thickness is 28 nm, and the real nanosheet thickness is 18 nm.

Evaluation of the optical band gap

The indirect band gap of the material was estimated by fitting the absorbance (α) to the Boltzmann function:[S1]

$$\alpha = \alpha_{max} + \frac{\alpha_{min} - \alpha_{max}}{1 + exp\left(\frac{E - E_0^{Boltz}}{\delta}\right)}$$

which takes into account the maximum (α_{max}) and minimum (α_{min}) values of absorbance in the region of fit and the energy E_0^{Boltz} corresponding to the mid-point between the limiting absorbance values. The fitting procedure resulted in the value of δ = 0.28 eV, from which the values of the direct and indirect band gaps were estimated as $E_g = E_0^{Boltz} - n\delta$, with n = 0.3 and 4.3, respectively.[S1] Correspondingly, the band gap values were estimated as E_g(direct) = 2.9 eV and E_g(indirect) = 1.8 eV.

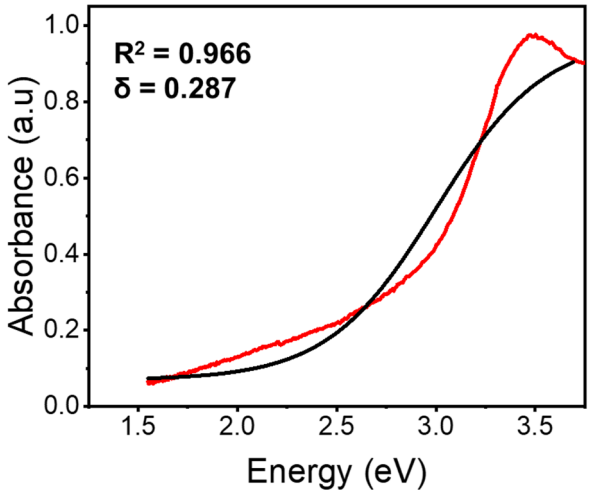

Figure S6. The absorbance spectrum of the $MnIn_2Se_4$ sheets collected at 7500 rpm (red curve). The black curve shows the fit to the Boltzmann function performed as explained below.

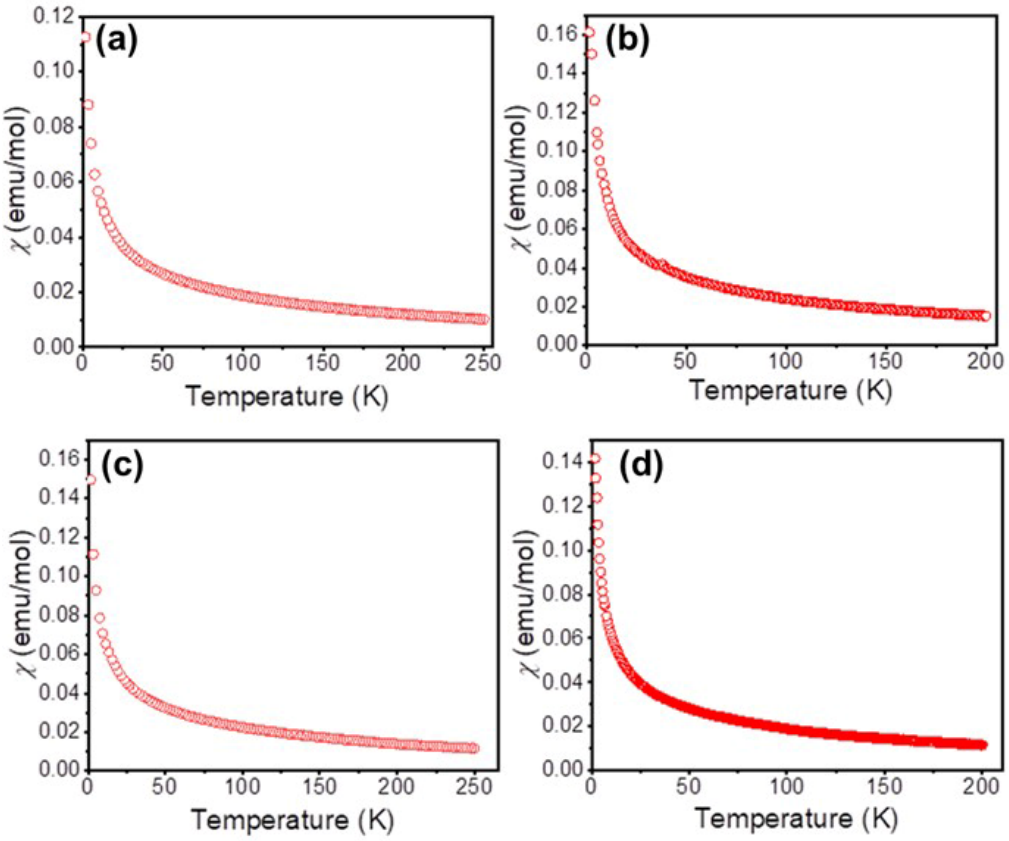

Figure S7. The temperature dependence of field-cooled magnetic susceptibility measured under applied field of 100 Oe for bulk $MnIn_2Se_4$ (a) and for the exfoliated sheets isolated at 2000 rpm (b), 5000 rpm (c), and 7500 rpm (d).

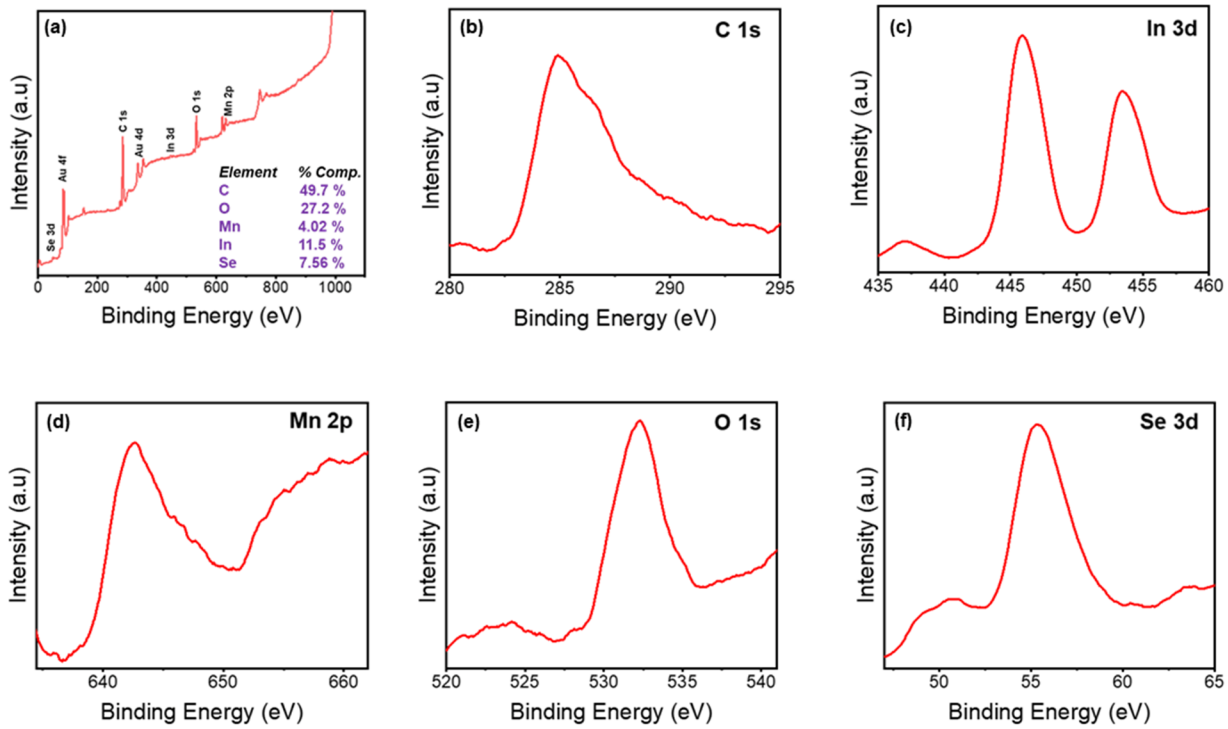

Figure S8. The XPS data recorded for the sheets collected at 2000 rpm (a) and spectral contribution of the individual elements (b-f). The spectra are dominated by C and O signals, due to the surfactant isopropanol and water molecules. Trace signals from Mn, In, and Se can be seen for the sheets collected at 2000 rpm, while XPS signals of these elements could be hardly detected for the thinner sheets collected at higher centrifugation speeds.

Calculations of the Mydosh parameter:

The Mydosh parameter (ϕ), used for the verification of spin-glass transition, was calculated as

$$\phi = \frac{T_{\max}^{\nu_1} - T_{\max}^{\nu_2}}{T_{\max}^{\nu_1}(\log \nu_1 - \log \nu_2)}$$

where $T_{\max}^{\nu_1}$ and $T_{\max}^{\nu_2}$ are the temperatures of the maximum in the in-phase magnetic susceptibility recorded at frequencies ν_1 and ν_2, respectively, of the applied AC magnetic field (Table S2). For a typical spin-glass material, $0.004 < \phi < 0.08$.[S2]

Table S2. Variation of the T_{cusp} (spin-freezing temperature) at different frequencies of the AC applied field.

Samples / AC Frequency →	1 Hz	10 Hz	100 Hz	1000 Hz
Bulk crystals	2.9 K	2.94 K	3.00 K	3.2 K
Sheets at 2000 rpm	2.7 K	2.8 K	2.82 K	2.91 K
Sheets at 5000 rpm	2.7 K	2.78 K	2.8 K	2.9 K

References

S1. R. A. Zanatta, Revisiting the optical bandgap of semiconductors and the proposal of a unified methodology to its determination. *Sci. Rep.*, 2019, **9**, 11225.

S2. Mydosh, J. A. Spin glasses: an experimental introduction; Taylor & Francis: Washington, DC, 1993.